RESEARCH PAPER

Purine receptor-mediated endocannabinoid production and retrograde synaptic signalling in the cerebellar cortex

Flora E. Kovacs[1], Peter Illes[2] and Bela Szabo[1]

[1]*Institut für Experimentelle und Klinische Pharmakologie und Toxikologie, Albert-Ludwigs-Universität, Freiburg i. Br., Germany, and* [2]*Rudolf-Boehm Institut für Pharmakologie und Toxikologie, Universität Leipzig, Leipzig, Germany*

BACKGROUND AND PURPOSE

Presynaptic CB_1 cannabinoid receptors can be activated by endogenous cannabinoids (endocannabinoids) synthesized by postsynaptic neurones. The hypothesis of the present work was that activation of calcium-permeable transmitter-gated ion channels in postsynaptic neurones, specifically of P2X purine receptors, can lead to endocannabinoid production and retrograde synaptic signalling.

EXPERIMENTAL APPROACH

GABAergic inhibitory postsynaptic currents (IPSCs) were recorded with patch-clamp techniques in Purkinje cells in mouse cerebellar slices. Purine receptors on Purkinje cells were activated by pressure ejection of ATP from a pipette.

KEY RESULTS

ATP evoked an inward current in Purkinje cells, most likely due to P2X receptor activation. The ATP-evoked currents were accompanied by currents via voltage-gated calcium channels. ATP suppressed electrical stimulation-evoked IPSCs and miniature IPSCs (mIPSCs) recorded in the presence of tetrodotoxin, and these effects were prevented by the CB_1 antagonist rimonabant and the calcium chelator BAPTA (applied into the Purkinje cell). ATP also suppressed mIPSCs when voltage-gated calcium channels were blocked by cadmium, and intracellular calcium stores were depleted by thapsigargin. However, ATP failed to suppress mIPSCs when the extracellular calcium concentration was zero.

CONCLUSIONS AND IMPLICATIONS

ATP elicits CB_1 receptor-dependent retrograde synaptic suppression, which is probably mediated by an endocannabinod released by the postsynaptic neurone. An increase in intracellular calcium concentration in the postsynaptic neurone is necessary for this retrograde signalling. We propose that ATP increases the calcium concentration by two mechanisms: calcium enters into the neurone via the P2X receptor ion channel and the ATP-evoked depolarization triggers voltage-gated calcium channels.

Abbreviations

ACSF, artificial cerebrospinal fluid; GABA, gamma aminobutyric acid; IPSC, inhibitory postsynaptic current; PRE, initial reference period; SOL, solvent

Introduction

The $G\alpha_{i/o}$ protein-coupled CB_1 cannabinoid receptor is probably the most abundant G protein-coupled receptor in the central nervous system. It is the primary neuronal target of the phytocannabinoid Δ^9-tetrahydrocannabinol and the endogenous cannabinoids (endocannabinoids; Howlett et al., 2002; Pertwee, 2005). Activation of CB_1 receptors leads to presynaptic inhibition of synaptic transmission in many regions of the central and peripheral nervous system (Freund et al., 2003; Szabo and Schlicker, 2005; Stephens, 2009).

Endocannabinoids and CB_1 receptors play an important physiological role in both short- and long-term synaptic plasticity. The basis of these actions is endocannabinoid-mediated retrograde signalling: endocannabinoids produced by postsynaptic neurones diffuse to presynaptic axon terminals and inhibit transmitter release by activating presynaptic CB_1 receptors (for review see Alger, 2002; Chevaleyre et al., 2006; Lovinger, 2008; Kano et al., 2009).

Two mechanisms are well established as triggers of endocannabinoid production in postsynaptic neurones. One mechanism triggering endocannabinoid production is activation of $G\alpha_{q/11}$ protein-coupled receptors. For example, activation of metabotropic glutamate receptors and muscarinic acetylcholine receptors by exogenous agonists leads to a calcium-independent endocannabinoid release and retrograde signalling (Maejima et al., 2001; Varma et al., 2001; Galante and Diana, 2004; Straiker and Mackie, 2007).

The second mechanism leading to endocannabinoid production is elevation of the intracellular calcium concentration. During depolarization-induced suppression of inhibition and depolarization-induced suppression of excitation, depolarization of postsynaptic neurones via the patch-clamp pipette leads to opening of voltage-gated calcium channels, and the resulting calcium influx triggers endocannabinoid production and subsequent endocannabinoid-mediated synaptic suppression (for example, Wilson and Nicoll, 2001; Wallmichrath and Szabo, 2002; Diana and Marty, 2003; Kim and Alger, 2004). Calcium increase occurring physiologically during action potential salvos can also trigger endocannabinoid production in postsynaptic neurones (Fortin et al., 2004; Brenowitz et al., 2006).

A combination of depolarization-elicited calcium influx with activation of $G\alpha_{q/11}$ protein-coupled receptors is an especially powerful trigger of endocannabinoid production, and occurs also physiologically during activation of glutamatergic synapses (Brown et al., 2003; Maejima et al., 2005; Marcaggi and Attwell, 2005; Rancz and Häusser, 2006).

The role of transmitter-gated ion channels (ionotropic receptors) in triggering endocannabinoid production and retrograde signalling is not well established. Several ionotropic receptors possess considerable calcium conductance [e.g. *N*-methyl-d-aspartate (NMDA)-type glutamate receptors, some nicotinic acetylcholine receptors and some P2X purine receptors], and therefore it can be assumed that calcium influx through these receptors can trigger endocannabinoid production. Indeed, it has recently been shown that activation of NMDA receptors can lead to calcium-dependent endocannabinoid production (Ohno-Shosaku et al., 2007).

The hypothesis of the present work was that activation of P2X purine receptors leads to calcium influx, endocannabinoid production and endocannabinoid-mediated retrograde synaptic signalling. We tested this hypothesis at inhibitory synapses of Purkinje cells of the cerebellar cortex. Purkinje cells possess several types of P2X receptors (Collo et al., 1996; Mateo et al., 1998; Rubio and Soto, 2001; Xiang and Burnstock, 2005). Our results are consistent with the following mechanism: activation of P2X purine receptors leads to calcium influx into the postsynaptic neurone via P2X receptor ion channels and voltage-gated calcium channels, and the calcium increase triggers endocannabinoid production and CB_1 receptor-mediated retrograde synaptic signalling.

Methods

The experiments conformed to the European Communities Council Directive of 24 November 1986 (86/609/EEC). All efforts were made to minimize the number of animals used and their suffering. The methods were similar to those described previously (Freiman et al., 2006; Szabo et al., 2006). The nomenclature for receptors and ion channels used in this work conforms to the 'Guide to receptors and channels' by the British Journal of Pharmacology (Alexander et al., 2009).

Brain slices

Eleven to 18-day-old Naval Medical Research Institute mice were anaesthetized with isoflurane (>3%) and decapitated. The brains were rapidly removed and placed in ice-cold artificial cerebrospinal fluid (ACSF) of the following composition (mM): NaCl 126, NaH_2PO_4 1.2, KCl 3, $MgCl_2$ 5, $CaCl_2$ 1, $NaHCO_3$ 26, glucose 20, Na-lactate 4, pH 7.3–7.4 (after the solution was gassed with 95% O_2/5% CO_2) and 250 µm thick sagittal slices of the cerebellar vermis were cut. After being cut, the slices were stored in a Gibb chamber containing ACSF of the following composition (mM): NaCl 126, NaH_2PO_4 1.2, KCl 3, $MgCl_2$ 1, $CaCl_2$ 2.5, $NaHCO_3$ 26, glucose 10, Na-lactate 4, pH 7.3–7.4. For patch-clamping, brain slices were superfused at a flow rate of 1.5 mL·min^{-1} with ACSF of the following composition (mM): NaCl 126, NaH_2PO_4 1.2, KCl 3, $MgCl_2$ 1, $CaCl_2$ 2.5, $NaHCO_3$ 26, glucose 10, pH 7.3–7.4. For the preparation of calcium-free ACSF, $CaCl_2$ was replaced by 3.75 mM NaCl. If not otherwise stated, the experiments were performed at 20–24°C, because patch-clamp recordings in brain slices are more stable at these temperatures.

Patch-clamping

Neurones in slices were visualized with infrared video microscopy, and patch-clamp recordings were obtained with an EPC-9 amplifier under the control of TIDA software (HEKA Elektronik, Lambrecht, Germany). Series resistance compensation of 50% was usually applied. Series resistance was measured before and after recordings and experiments with major changes in series resistance (>20%) were discarded. GABAergic synaptic events were recorded in the presence of the NMDA and non-NMDA glutamate receptor antagonists DL-AP5 (2.5×10^{-5} M) and DNQX (10^{-5} M) at a holding potential of –70 mV with pipettes (2.5–5 MΩ) containing (mM): CsCl 147, $MgCl_2$ 1, HEPES 10,

glycol-bis(2-aminoethylether)-N,N,N',N'-tetraacetic acid, ATP-Na$_2$ 4, GTP-Na 0.4, N-ethyl-lidocaine Cl 2, pH 7.4. Electrically evoked inhibitory postsynaptic currents (eIPSCs) were evoked by stimulating pipettes (filled with ACSF) inserted into the molecular layer. Miniature inhibitory postsynaptic currents (mIPSCs) were recorded in the presence of tetrodotoxin (3×10^{-7} M), and cadmium spontaneous IPSCs (sIPSCs) were recorded in the presence of cadmium (10^{-4} M). ATP was pressure ejected from a pipette positioned above the surface of the slice. Pressure pulses (30–45 kPa pressure; 5 s duration) were delivered by a Picopump 820 (World Precision Instruments, Berlin, Germany).

Fluorescence measurement of calcium concentrations in Purkinje cells

In addition to the intracellular solution used for recording postsynaptic currents, the patch pipette contained the low-affinity calcium indicator Oregon green 488 BAPTA-5N (K_d for calcium, 2×10^{-5} M; final concentration, 2×10^{-4} M). Fluorescence intensity in Purkinje cells was determined with an imaging system consisting of: Polychrome IV monochromatic light source, a cooled IMAGO VGA CCD camera and TILLvision imaging software (TILL Photonics, Gräfelfing, Germany). Fluorescence changes were evaluated in regions of interest. Fluorescence values were corrected for background fluorescence. For further evaluation, ratios between stimulation-evoked fluorescence changes (ΔF) and baseline fluorescence measured immediately before stimulation (F_0) were calculated ($\Delta F/F_0$ ratios).

Protocols and statistics

Recordings were started 15 (electrophysiological recordings) or 30 min (calcium imaging) after establishment of the whole-cell configuration. mIPSCs and cadmium sIPSCs were detected with the MiniAnalysis software (version 6.0.1; Synaptosoft, Decatur, GA, USA). Amplitude and frequency values of mIPSCs and cadmium sIPSCs were transferred from Mini-Analysis to Sigmaplot (SPSS, Chicago, IL, USA), and further calculations were performed by a program written by us in Sigmaplot. This program calculated, for example, the cumulative amplitude of mIPSCs and cadmium sIPSCs by summing up the amplitudes of all mIPSCs and cadmium sIPSCs within 10-s periods. Accordingly, the cumulative amplitude reflects changes both in frequency and in amplitude. ATP-evoked changes in synaptic transmission were quantified by expressing eIPSC amplitude and mIPSC and cadmium sIPSC parameters (frequency, amplitude and cumulative amplitude) as percentages of initial reference values (PRE in the figures). Means $\pm$ standard error of the mean are given throughout. Non-parametric statistical tests were used to identify significant differences. The two-tailed Mann–Whitney test was used for comparisons between groups; significant differences are indicated by *. The two-tailed Wilcoxon signed rank test was used for comparisons within groups (vs. PRE); significant differences are indicated by black symbols or by #. $P < 0.05$ was taken as the limit of statistical significance, and only this level is indicated, even if P was <0.01 or <0.001.

Drugs

Drugs were obtained from the following sources. From Sanofi-Aventis (Chilly-Mazarin, France), rimonabant (previously called SR141716A); Sigma Aldrich (Deisenhof, Germany): adenosine 5′-triphosphate disodium salt (ATP), adenosine 5′-diphosphate sodium salt (ADP), ethylenedioxybis(o-phenylenenitrilo)tetraacetic acid (BAPTA), uridine 5′-triphosphate TRIS salt (UTP), guanosine 5′-[γ-thio]triphosphate tetralithium salt (GTPγS), guanosine 5′-triphosphate sodium salt (GTP), cadmium chloride (CdCl$_2$), bicuculline and ivermectin; Ascent Scientific (Weston, UK): 6,7-dinitroquinoxaline-2,3-dione (DNQX), DL-(-)-2-amino-5-phosphonopentanoic acid (DL-AP5) (E)-ethyl 1,1a,7,7a-tetrahydro-7-(hydroxyimino)cyclopropa[b]chromene-1a-carboxylate, 4-[[4-formyl-5-hydroxy-6-methyl-3-[(phosphonooxy)methyl]-2-pyridinyl]azo]-1,3-benzenedisulphonic acid tetrasodium salt (PPADS) (E)-Ethyl 1,1a,7,7a-tetrahydro-7-(hydroxyimino) cyclopropa[b]chromene-1a-carboxylate (CPCCOEt) (RS)-3,5-dihydroxyphenylglycine (DHPG); Biotrend (Köln, Germany): 6-N,N-diethyl-D-β,γ-dibromomethyleneATP trisodium salt (ARL 67156); Alamone Laboratories (Jerusalem, Israel): N-ethyl-lidocaine chloride (QX-314), thapsigargin; Invitrogen (Leiden, the Netherlands): Oregon green 488 BAPTA-5N hexapotassium salt.

Rimonabant, DNQX, bicuculline and ivermectin were dissolved in dimethylsulphoxide (DMSO), and stock solutions were stored at –32°C. Further dilutions were made with superfusion buffer; the final concentration of DMSO in the superfusion fluid was ≤1 mL·L^{-1} (except in the case of ivermectin 10^{-4} and 5×10^{-5} M, 2 mL·L^{-1} DMSO). Control solutions ('SOL' in the figures) always contained the appropriate concentrations of DMSO.

Results

ATP responses in Purkinje cells

Purkinje cells in the cerebellar cortex were patch-clamped. Because it is known that P2X purine receptors desensitize rapidly (Nörenberg and Illes, 2000; North, 2002), we decided to apply ATP only for short periods by pressure-ejecting the substance from a pipette (10^{-2} M ATP in the pipette; ~5 μm pipette opening; <0.05 μL ejection volume). The ejection pipette was positioned 20–30 μm above the brain slice and above the dentritic tree of the patch-clamped Purkinje cell. We believe that due to dilution in the superfusion buffer, the concentration of ATP at the target Purkinje cells was much lower than the concentration in the ejection pipette (but see also Di Angelantonio and Nistri, 2001 for the dilution of drugs after pressure application). ATP elicited an inward current of 1226 ± 180 pA ($n = 5$) amplitude (Figure 1A1), and this current will be termed 'purinergic current'. The purinergic current was accompanied by several calcium spikes (Figure 1A1). The fluorometrically determined intracellular calcium concentration increased markedly in the soma and even more in the dendrites (Figure 1A2 and A3).

Superfusion of cadmium (10^{-4} M), an inhibitor of several types of voltage-gated calcium channels, abolished the calcium spikes, as expected (Figure 1B1). In the presence of cadmium, the amplitude of the purinergic current was 1238 ± 162 pA ($n = 5$). Thus, cadmium did not affect the purinergic current (compare Figure 1B1 with Figure 1A1). Cadmium significantly inhibited the ATP-evoked calcium concentration increase in the dendrites (compare Figure 1B3 with
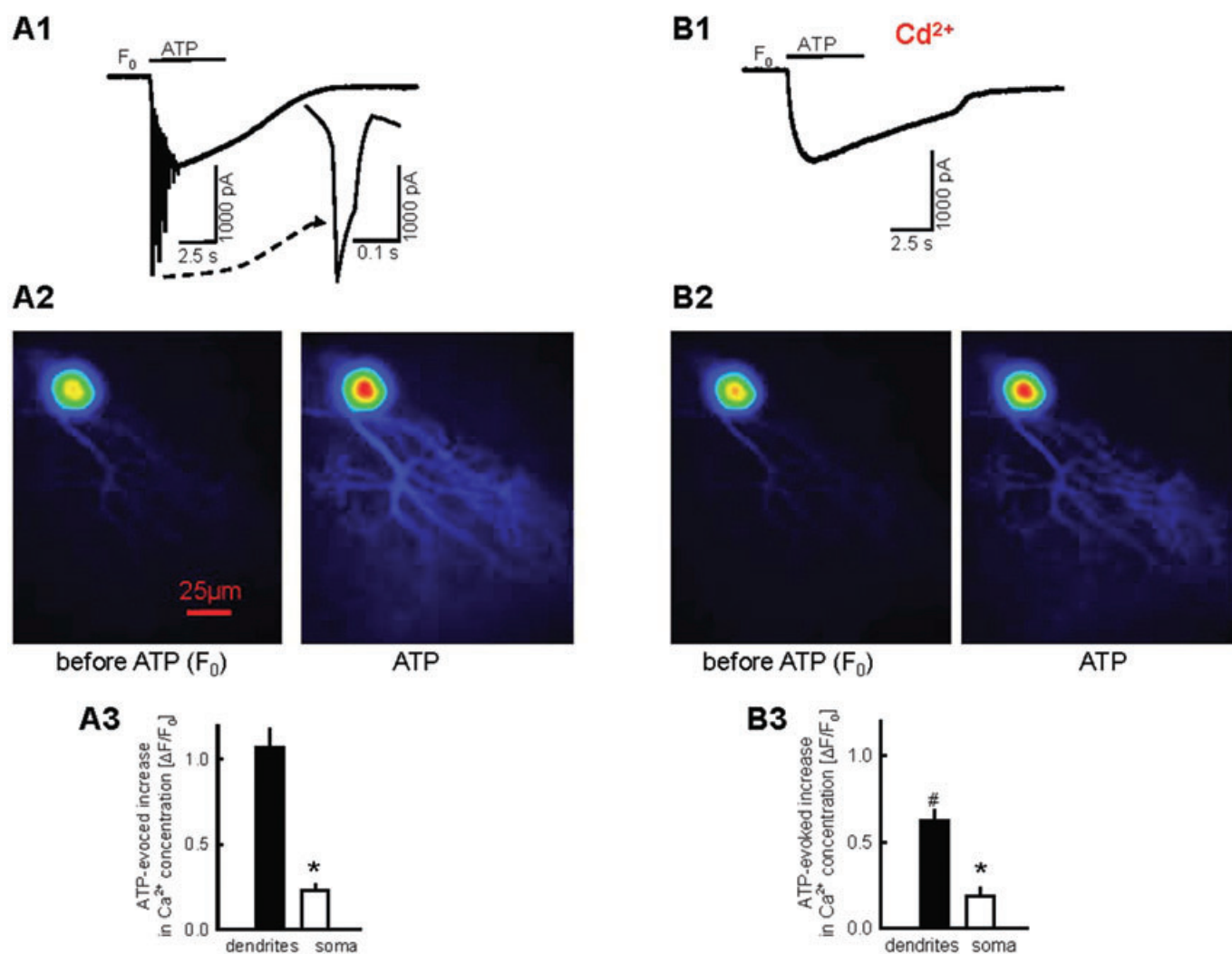
Figure 1

ATP responses in Purkinje cells. Glutamatergic and GABAergic synaptic input to Purkinje cells was blocked by DNQX, AP5 and bicuculline, and the patch-clamp pipette contained the calcium-sensitive fluorescent dye Oregon green 488 BAPTA-5N. (A1) Pressure ejection of ATP from a pipette elicited an inward current ('purinergic current') which was accompanied by several calcium spikes (a calcium spike is shown with higher temporal resolution). (A2) The fluorescent images and the (A3) statistical evaluation of calcium concentration changes indicate that ATP increased the calcium concentration in the soma and the dendrites. (B1-B3) ATP responses of the neurones shown in (A1-A3) during cadmium (10^{-4} M) superfusion. Means $\pm$ standard error of the mean of five experiments. Currents and calcium concentrations were recorded in the same neurones. * Indicates significant difference versus dendrite ($P < 0.05$). # Indicates significant difference ($P < 0.05$) versus $\Delta F/F_0$ in the absence of cadmium (shown in A3).

Figure 1A3). Importantly, ATP elicited a calcium concentration increase in the Purkinje cells also when voltage-gated calcium channels were blocked (Figure 1B3).

Sodium currents were not observed during ATP application, because the patch-clamp pipette contained N-ethyl-lidocaine, an inhibitor of voltage-gated sodium channels. Voltage-gated sodium channels are anyhow only very weakly expressed in the dendritic tree of Purkinje cells (Lasser-Ross and Ross, 1992; Stuart and Häusser, 1994).

Characterization of the current elicited by ATP in Purkinje cells

Next, we aimed to identify the receptor activated by ATP. ATP is rapidly transformed by ecto-nucleotidases in the brain into

ADP, AMP and adenosine (Illes *et al.*, 1996; Zimmermann, 1996; Ralevic and Burnstock, 1998). ATP itself is an agonist of transmitter-gated P2X receptors and of the G protein-coupled P2Y receptors (Abbracchio and Burnstock, 1994; Fredholm *et al.*, 1997). ADP is an agonist at P2Y receptors, whereas adenosine activates adenosine (A) receptors (Klotz, 2000; Abbracchio *et al.*, 2006; Burnstock, 2007). As a first step, we wanted to determine whether ATP acted itself, or acted via its degradation products ADP and adenosine (Figure 2A). ATP was pressure ejected four times. The superfusion of solvent or the ecto-nucleotidase inhibitor ARL67156 (5×10^{-5} M; Brock-haus *et al.*, 2004) started after the second ATP application. The purinergic current remained stable in the solvent-superfused slices (Figure 2A). This observation verifies that the short pressure-ejection of ATP did not lead to
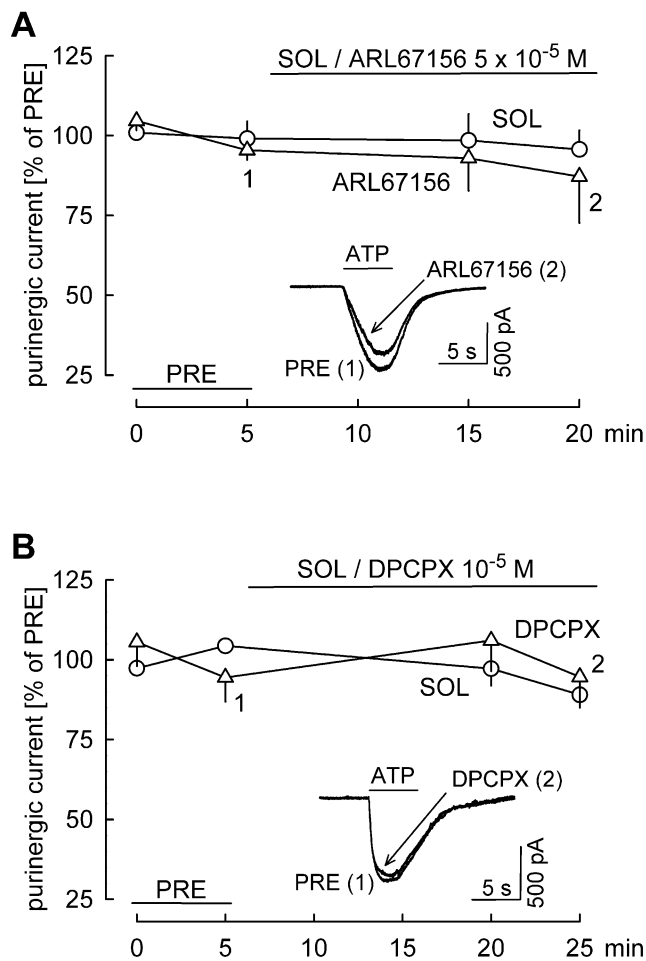
Figure 2

ATP acts itself and A1 adenosine receptors are not involved in the effects of ATP. In addition to DNQX, AP5 and bicuculline, cadmium was added to the superfusion ACSF to block voltage-gated calcium channels. ATP was pressure ejected from a pipette four times. Amplitudes of ATP-evoked currents were expressed as percentages of the initial reference value PRE. Shown are means ± standard error of the mean. (A) After the second ATP application, solvent (SOL; $n = 3$) or the ecto-nucleotidase inhibitor ARL67156 ($n = 8$) was superfused. The original tracings were recorded in a slice with ARL67156 superfusion at time points 1 and 2. (B) After the second ATP application, solvent (SOL; $n = 3$) or the A1 receptor antagonist DPCPX ($n = 4$) was superfused. The original tracings were recorded in a slice with DPCPX superfusion at time points 1 and 2.

desensitization of the receptor involved. The ecto-nucleotidase inhibitor also did not change the purinergic current (Figure 2A), indicating that ATP itself elicited the current, there was no need for its conversion into ADP or adenosine. Because ATP does not directly activate A_1 adenosine receptors, this observation argues against a role for A_1 receptors in the purinergic current.

To assess more exactly the role of the A_1 receptor in the ATP-evoked current, we performed experiments with the A_1 receptor antagonist DPCPX (Figure 2B). As in the previous series, ATP was pressure ejected four times. After the second ATP application, solvent or DPCPX was superfused. The puri-

nergic current was not changed in either group (Figure 2B), indicating that A_1 receptors were not involved in the ATP-evoked purinergic current.

For advancing the identification of the receptor involved in the ATP effect, we determined whether G protein-coupled receptors were involved in the ATP effect (Figure 3). To this aim, we tested the effect of GTPγS, applied via the patch-clamp pipette intracellularly. In the presence of this non-hydrolysable ATP analogue, G protein activation triggered by the first agonist application becomes long-lasting, and subsequent agonist applications trigger only moderate, if any, G protein activation (e.g. Jeong et al., 2001). At first, we carried out positive-control experiments. In one group, GTP was included in the patch clamp pipette, and the mGluR agonist DHPG (10^{-5} M) was pressure ejected three times (Figure 3A). DHPG elicited an inward current as described previously (e.g. Kim et al., 2003), and the charge transfer (area under the current curve) was identical during the three DHPG applications. The DHPG current was abolished by the mGluR1 antagonist CPCCOEt, verifying involvement of mGluR1 receptors (not shown). The pattern of effects of DHPG was different in neurones patched with pipettes containing GTPγS. The effect of the first DHPG application was prolonged, resulting in higher charge transfer values, and the second and third DHPG application elicited only small charge transfers (Figure 3A). The results show that GTPγS enhances the first effect elicited by activation of a G protein-coupled receptor and attenuates later effects. Then, we tested the interaction between pressure-ejected ATP and GTPγS in the patch pipette (Figure 3B). In neurones with GTP in the pipette, ATP elicited identical currents, when applied three times. The picture did not change in the presence of GTPγS in the pipette, suggesting that G protein-coupled receptors were not involved in the purinergic currents.

For obtaining further information on the properties of the receptor activated by ATP, we compared the effects of ATP, ADP and UTP. Ejection pipettes were filled with equimolar concentrations (10^{-2} M) of ATP, ADP and UTP. ATP, ADP and UTP elicited inward currents of 1046 ± 73 pA ($n = 16$), 75 ± 39 pA ($n = 10$) and 214 ± 49 pA ($n = 13$) amplitude, respectively. Thus, the currents elicited by ADP and UTP were much smaller than the current elicited by an equimolar concentration of ATP (the differences were also statistically significant; $P < 0.05$). This observation argues against the involvement of P2Y receptors in the ATP effect, because ATP has a lower or similar affinity for P2Y receptors than ADP and UTP (Ralevic and Burnstock, 1998; Burnstock, 2007). On the other hand, it is known that ATP possesses much higher affinity for several P2X receptors than ADP and UTP. Thus, the pattern of effects of the three nucleotides is compatible with an involvement of P2X receptors in the ATP-evoked current.

The interaction between PPADS (10^{-4} M) and ATP was also tested (Supporting Information Figure S1). PPADS is a mixed purine receptor antagonist, which blocks $P2X_{1,2,3,5}$ receptors and some P2Y receptors (especially $P2Y_1$) (Buell et al., 1996; Lambrecht, 2000; von Kügelgen, 2006; Jarvis and Khakh, 2009). The behaviour of PPADS at the mouse $P2X_4$ receptor is not clear. In one study (Jones et al., 2000), PPADS was found to be an antagonist with low potency, whereas in another study (Townsend-Nicholson et al., 1999), PPADS even potentiated $P2X_4$ receptor-mediated responses evoked by ATP. In
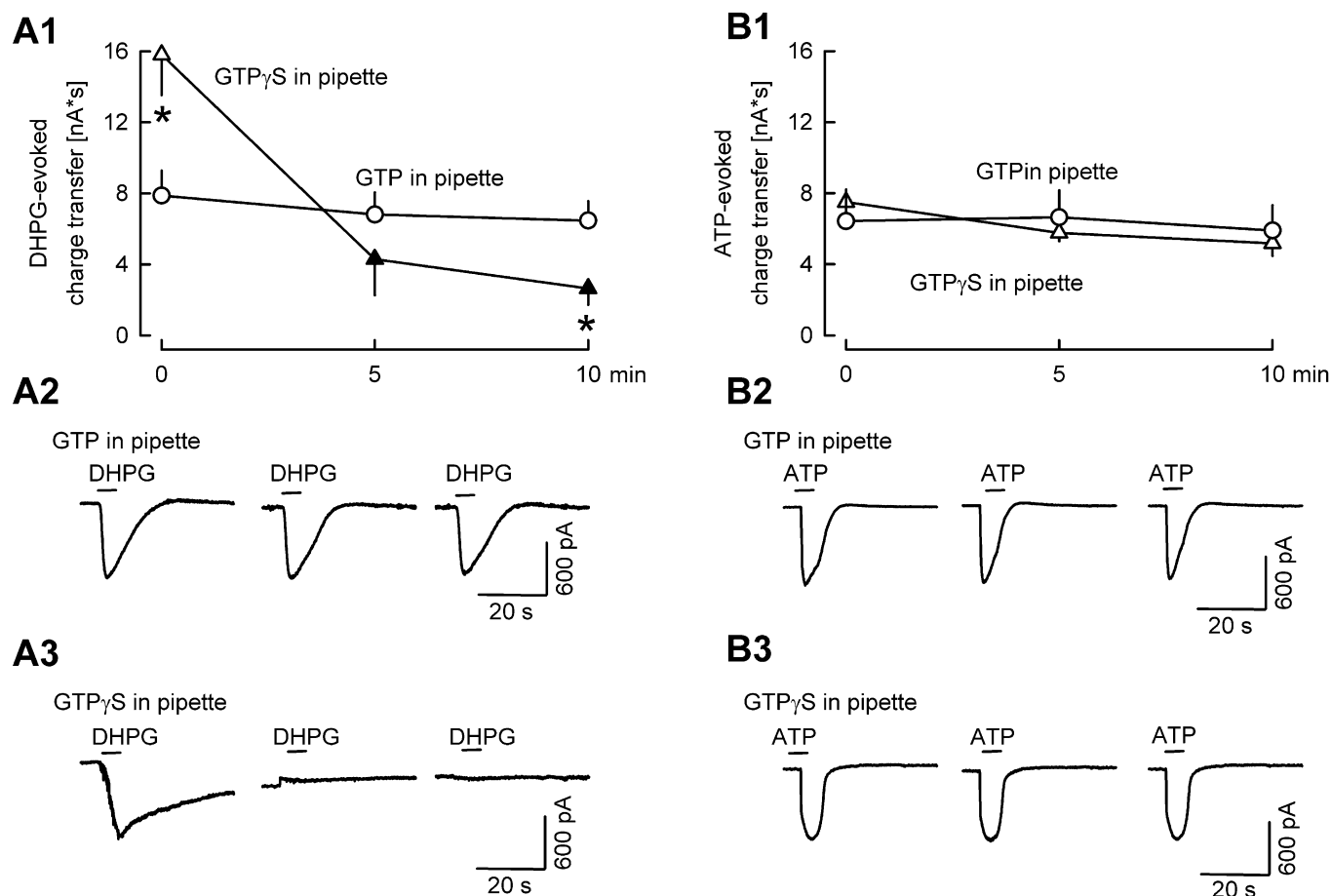
Figure 3

The stable ATP analogue GTPγS does not affect the pattern of ATP-evoked currents. In addition to DNQX, AP5 and bicuculline, cadmium was added to the superfusion ACSF to block voltage-gated calcium channels. The patch clamp pipette contained GTP or GTPγS. (A) The mGluR agonist DHPG was pressure ejected from a pipette three times. In the presence of GTP in the patch-clamp pipette ($n = 7$), the DHPG-evoked charge transfer remained constant (charge transfer was calculated for the 50-s period following DHPG application). GTPγS in the patch-clamp pipette ($n = 7$) prolonged the effect of the first DHPG application (thereby increasing charge transfer), and diminished the effects of the further DHPG applications. * Indicates significant difference from GTP ($P < 0.05$). (A2-A3) Original tracings of DHPG-evoked currents in the presence of GTP or GTPγS. (B) ATP was pressure ejected from a pipette three times. In the presence of GTP in the patch-clamp pipette ($n = 5$), the ATP-evoked charge transfer remained constant (charge transfer was calculated for the 50-s period following ATP application). The ATP effect was similar in experiments with GTPγS in the patch-clamp pipette ($n = 5$). (B2-B3) Original tracings of purinergic currents in the presence of GTP or GTPγS.

our study, two concentration-response curves for pressure-ejected ATP were determined in one experiment. If the solvent of PPADS was superfused during the second concentration–response curve, the curve was essentially identical with the first concentration–response curve (supporting Figure S1A). PPADS also did not affect the concentration–response curve of ATP (supporting Figure S1B). These results argue against the involvement of a series of purine receptors, which are sensitive to PPADS, namely $P2X_{1,2,3,5}$ and P2Y1 receptors. The results are compatible with the involvement of PPADS-insensitive receptors, for example, the $P2X_4$ receptor.

Finally, we tested the effect of ivermectin on ATP-evoked currents (Figure 4). Ivermectin is known to prolong $P2X_4$ receptor-mediated effects (Gever *et al.*, 2006). When ATP was pressure ejected four times in the presence of the solvent of ivermectin, the amplitude and duration of the evoked currents remained constant; therefore, charge transfer via the

neuronal membrane remained constant (Figure 4A1). Ivermectin 10^{-6} M and 10^{-5} M also did not affect the ATP-evoked currents. Ivermectin 5×10^{-5} M slightly potentiated the ATP response. At the highest concentration, 10^{-4} M, ivermectin strongly potentiated the ATP-evoked current (Figure 4A1), and this potentiation was mostly due to the prolongation of the ATP effect with little change in the amplitude (Figure 4A2). The potentiation of the ATP effect by ivermectin suggests that $P2X_4$ receptors play a role in its action.

Effect of ATP on GABAergic synaptic transmission

Our main aim was to test whether activation of P2X receptors leads to endocannabinoid production and endocannabinoid-mediated suppression of GABAergic synaptic transmission. In the first series of experiments, eIPSCs were elicited every 20 s by electrical stimulation of GABAergic axons in the vicinity of
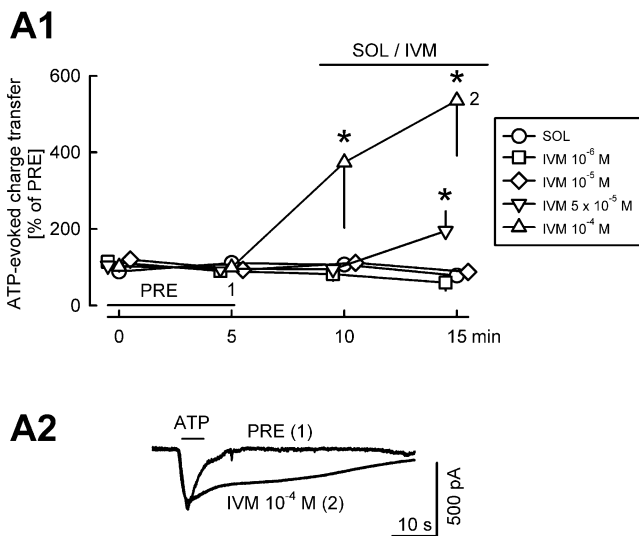
A1

A2

Figure 4

Ivermectin potentiates ATP-evoked currents. In addition to DNQX, AP5 and bicuculline, cadmium was added to the superfusion ACSF to block voltage-gated calcium channels. ATP was pressure ejected from a pipette four times. After the second ejection, solvent (SOL) or ivermectin (IVM) was superfused. ATP-evoked charge transfer values were expressed as percentages of the initial reference value PRE. Means $\pm$ standard error of the mean of seven (SOL), three (IVM 10^{-6} M), three (IVM 10^{-5} M), six (IVM 5×10^{-5} M) and four (IVM 10^{-4} M) experiments. * Indicates significant difference from SOL ($P < 0.05$). (A2) The original tracings were recorded in a slice with IVM 10^{-4} M superfusion at time points 1 and 2 (indicated in A1).

patch-clamped Purkinje cells, and ATP was pressure-ejected from a pipette twice (Figure 5). ATP evoked purinergic currents and calcium spikes, similar to those depicted in Figure 1A (not shown). In the presence of solvent, ATP suppressed the eIPSCs (Figure 5). When the experiments were performed in the presence of the CB_1 receptor antagonist rimonabant (10^{-6} M), ATP failed to suppress eIPSCs (Figure 5). These results suggest that ATP evoked an endocannabinoid- and CB_1 receptor-mediated suppression of GABAergic synaptic transmission.

To analyse the mechanism of the suppression of GABAergic synaptic transmission by ATP, we investigated the effect of ATP on miniature IPSCs (mIPSCs). mIPSCs were isolated by the inclusion of tetrodotoxin in the superfusion medium (Figure 6). Pressure-ejected ATP evoked strong purinergic currents in these experiments (966 $\pm$ 80 pA; $n = 34$), and these currents triggered additional calcium spikes (see Figure 6D). In solvent-treated slices, ATP lowered the frequency of mIPSCs (Figure 6A), whereas the amplitude of mIPSCs was not changed (Figure 6B). Corresponding to these changes in the primary parameters, the cumulative amplitude of mIPSCs was also lowered (Figure 6C). ATP-evoked changes in mIPSC properties were also analysed by constructing cumulative probability distribution plots of mIPSC amplitudes and inter-event intervals (supporting Figure S2). ATP did not cause a significant shift in the distribution of mIPSC amplitudes. However, ATP caused a significant shift of the distribution plot of mIPSC inter-event intervals to the direction of lower
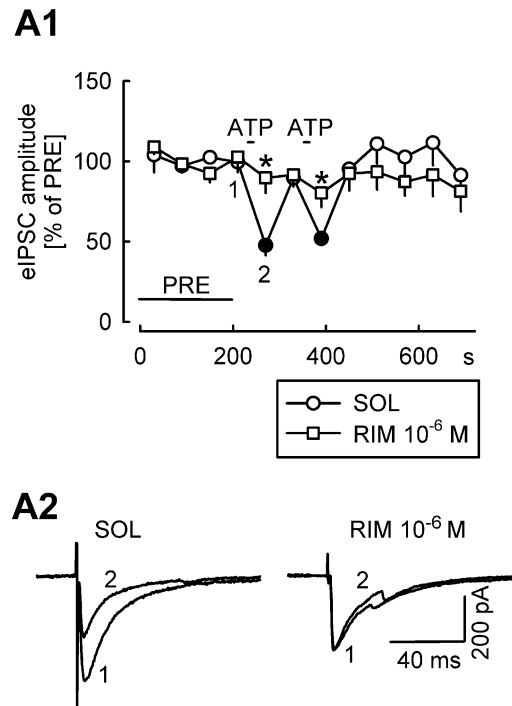
A1

A2

Figure 5

ATP suppresses electrically evoked inhibitory postsynaptic currents (eIPSCs). DNQX and AP5 were present in the superfusion ACSF. eIPSCs were elicited every 20 s by electrical stimulation in the molecular layer. Every three eIPSCs were averaged and expressed as percentages of eIPSCs during the initial reference period PRE. Pressure ejection of ATP evoked purinergic currents which were accompanied by calcium spikes (not shown). The points after ATP application are the averages of three eIPSCs elicited 5, 25 and 45 s after the 5-s ATP application. Means $\pm$ standard error of the mean of 9 (SOL) and 10 (RIM) experiments. Filled symbols indicate significant difference versus the time point preceding ATP ejection ($P < 0.05$); * Indicates significant difference from SOL ($P < 0.05$). (A2) The original tracings were recorded at time points 1 and 2 (indicated in A1) in the presence of solvent or rimonabant.

frequencies. The decrease in mIPSC frequency by ATP directly points to a presynaptic inhibitory mechanism. The lack of effect of ATP on the amplitude of mIPSCs indicates that there was no postsynaptic influence on the synaptic current, and is an indirect proof of the presynaptic action. In the presence of rimonabant (10^{-6} M), ATP no longer lowered the frequency and cumulative amplitude of mIPSCs (Figure 6A, C), verifying the involvement of endocannabinoids and CB_1 receptors.

Our next aim was to clarify the involvement of calcium in the ATP-evoked suppression of GABAergic transmission. In a first series of experiments, we included a high concentration of the fast calcium chelator BAPTA (4×10^{-2} M) in the pipette used for patch-clamping the postsynaptic Purkinje cells, and mIPSCs were recorded in the presence of tetrodotoxin (Supporting Information Figure S3). Pressure-ejected ATP evoked strong purinergic currents in these experiments (1011 $\pm$ 59 pA; $n = 34$), and these currents triggered additional calcium spikes (see Supporting Information Figure S3D). Irrespective of whether the experiments were performed in the
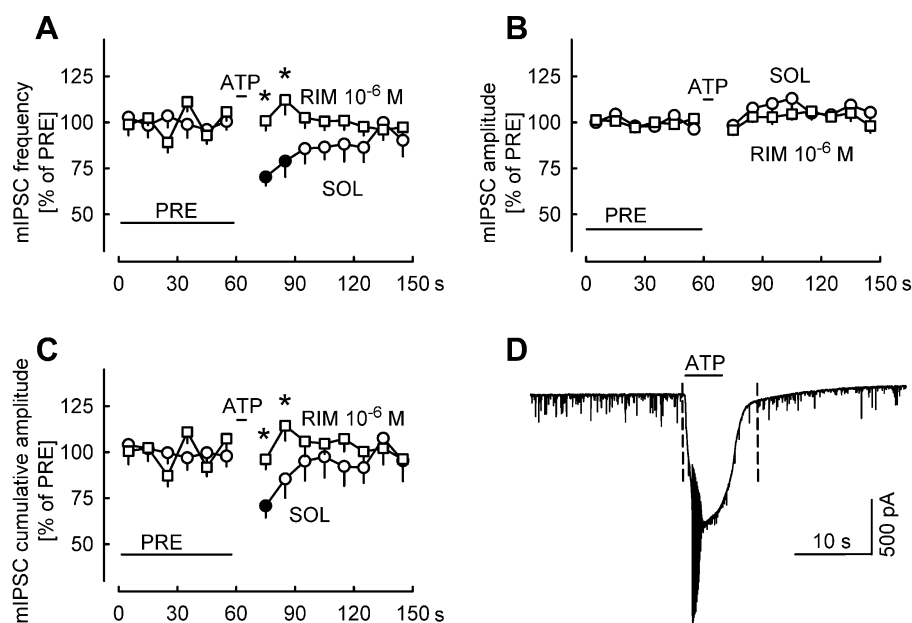
Figure 6

ATP suppresses miniature inhibitory postsynaptic currents (mIPSCs) recorded in the presence of tetrodotoxin. In addition to DNQX and AP5, tetrodotoxin (3×10^{-7} M) was present in the superfusion ACSF to block voltage-gated sodium channels. (A–C) The frequency, amplitude and cumulative amplitude of mIPSCs were evaluated in 10-s periods and expressed as percentages of values during the initial reference period PRE. Pressure ejection of ATP evoked purinergic currents which were accompanied by calcium spikes (see D). Means ± standard error of the mean of 16 (SOL) and 18 (RIM) experiments. Filled symbols indicate significant difference versus PRE ($P < 0.05$); * indicates significant difference from SOL ($P < 0.05$). (D) An original tracing recorded in the presence of solvent (the period between the dashed lines was not evaluated in A-C).

presence of solvent or rimonabant (10^{-6} M), ATP did not cause any change in mIPSCs: the frequency, amplitude and cumulative amplitude of mIPSCs remained constant (Supporting Information Figure S3A, B and C). These results indicate that an increase in intracellular calcium concentration is necessary for the CB_1 receptor-mediated retrograde signalling elicited by ATP.

In the last part of our study, we wanted to determine the source of calcium ions triggering endocannabinoid production during the application of ATP. Three sources were considered: calcium influx through P2X receptor channels (our initial hypothesis), calcium influx through voltage-gated calcium channels and calcium release from intracellular stores.

At first, we wanted to verify that calcium influx from the extracellular space into Purkinje cells contributes to the ATP-evoked purinergic current and increase in intracellular calcium concentration. Combined patch-clamp and fluorometric calcium imaging experiments were performed (Figure 7). Experiments were carried out in the presence of the broad-spectrum voltage-gated calcium channel inhibitor cadmium (10^{-4} M) and the sarcoplasmic reticulum calcium ATPase (SERCA) inhibitor thapsigargin (10^{-5} M). ATP was pressure ejected at first in the presence ACSF with normal calcium concentration (2.5 mM) and then in the presence of calcium-free ACSF. During superfusion of the calcium-containing ACSF, ATP evoked a purinergic current of 1275 ± 137 pA ($n = 4$) amplitude (Figure 7A1), and increased the calcium concentration in the dendrites and soma of the

Purkinje cells (Figure 7A2, A3). During superfusion of calcium-free ACSF, the amplitude of the ATP-evoked purinergic current significantly ($P < 0.05$) decreased to 476 ± 82 pA ($n = 4$) (compare Figure 7B1 with A1). The ATP-evoked increase in intracellular calcium concentration in the dendrites was also greatly attenuated (compare Figure 7B2, B3 with A2, A3). Thus, calcium influx from the extracellular space into Purkinje cells contributes to the ATP-evoked purinergic current and increase in intracellular calcium concentration.

Subsequently, we wished to clarify whether ATP is able to suppress GABAergic transmission when calcium influx through voltage-gated calcium channels and calcium release from intracellular stores are both inactivated (Figure 8). Experiments were carried out in the presence of the voltage-gated calcium channel inhibitor cadmium (10^{-4} M) and the SERCA inhibitor thapsigargin (10^{-5} M). Cadmium acts not only on postsynaptic Purkinje cells, but also blocks voltage-gated calcium channels in the axon terminals of inter-neurones, thereby eliminating sIPSCs elicited by action potentials and subsequent activation of voltage-gated calcium channels. It was shown that in cerebellar Purkinje cells cadmium isolates the same set of GABAergic synaptic events which are also isolated by the sodium channel inhibitor tetrodotoxin (see Than and Szabo, 2002). For clarity, the GABAergic synaptic events recorded in the presence of cadmium will be termed as 'cadmium sIPSCs'. Pressure-ejected ATP evoked strong purinergic currents in these experiments (1183 ± 67 pA; $n = 34$), but no calcium spikes occurred

A1

Cd²⁺ + thapsigargin; Ca²⁺ₒ = 2.5 mM

A2

before ATP (F₀)　　　ATP

A3

B1

Cd²⁺ + thapsigargin; Ca²⁺ₒ = 0 mM

B2
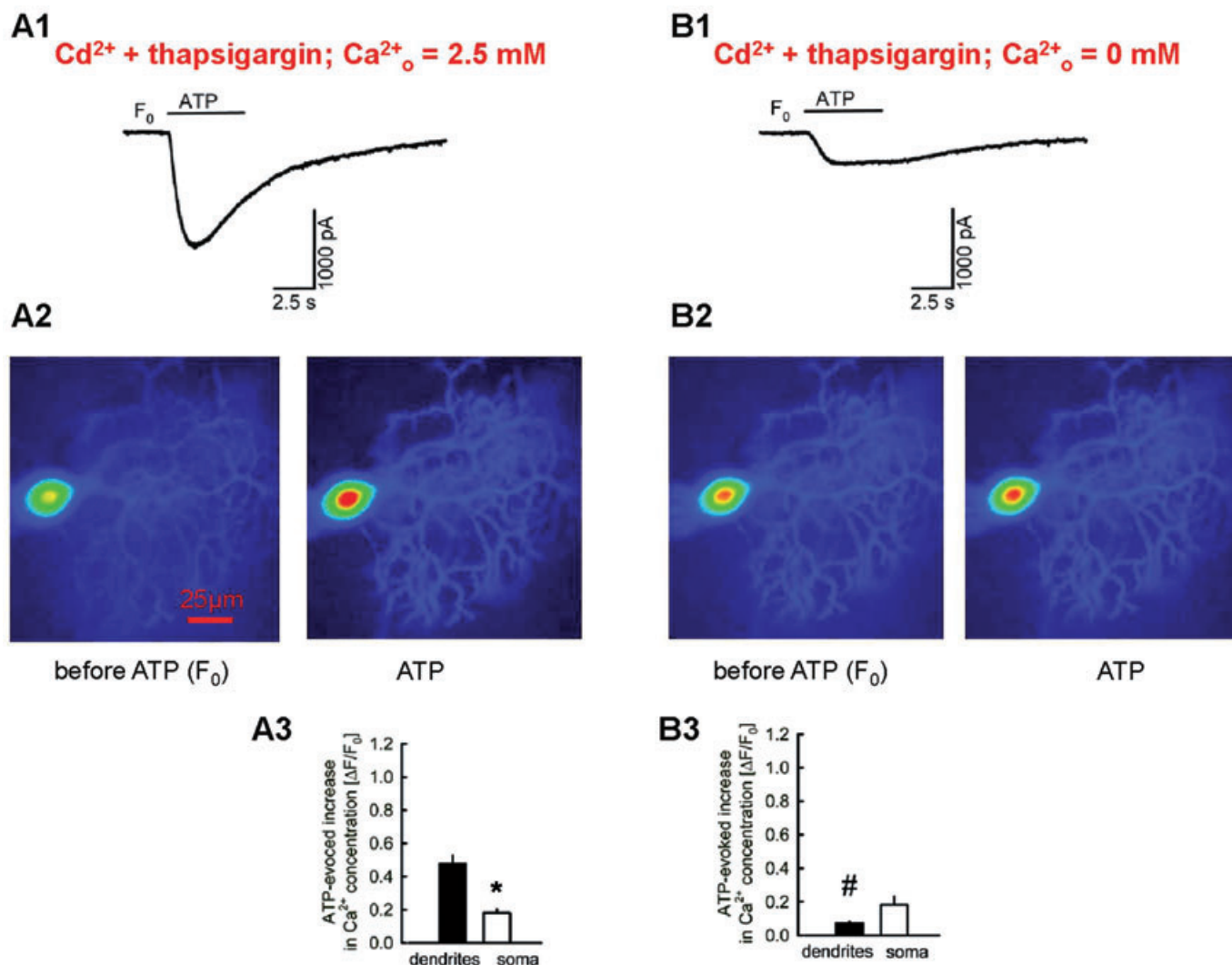

before ATP (F₀)　　　ATP

B3

Figure 7

Superfusion with calcium-free artificial cerebrospinal fluid (ACSF) diminishes the ATP-evoked current and the increase in intracellular calcium concentration. Glutamatergic and GABAergic synaptic input to Purkinje cells was blocked by DNQX, AP5 and bicuculline, and the patch-clamp pipette contained the calcium-sensitive fluorescent dye Oregon green 488 BAPTA-5N. The entire experiment was performed in the presence of cadmium (10^{-4} M) and thapsigargin (10^{-5} M). (A1) Pressure ejection of ATP from a pipette elicited a strong purinergic current. (A2) The fluorescent images and the (A3) statistical evaluation of calcium concentration changes indicate that ATP increased the calcium concentration in the soma and the dendrites. (B1-B3) ATP responses of the neurones shown in A1–A3 during superfusion with calcium free ACSF ($Ca^{2+}_o = 0$ mM). Means ± standard error of the mean of four experiments. Currents and calcium concentrations were recorded in the same neurones. * Indicates significant difference versus dendrite ($P < 0.05$). # Indicates significant difference ($P < 0.05$) versus $\Delta F/F_0$ in the presence of calcium in the ACSF (shown in A3).

due to cadmium (see Figure 8D). ATP suppressed the frequency and cumulative amplitude of cadmium sIPSCs (Figure 8A, C), without influencing their amplitude (Figure 8B). In the presence of rimonabant (10^{-6} M), ATP no longer suppressed the frequency and cumulative amplitude of cadmium sIPSCs (Figure 8A, C). These experiments show that ATP can evoke endocannabinoid-mediated retrograde suppression of GABAergic transmission in the absence of operation of voltage-gated calcium channels and calcium release from intracellular stores. A likely source of calcium in this condition is calcium entry through P2X receptor channels.

Finally, in the same experiments, we studied the role of calcium influx from the extracellular space into Purkinje cells in the suppression of synaptic transmission (Figure 9). Cadmium (10^{-4} M) and thapsigargin (10^{-5} M) were still present in the ACSF, but the ACSF was nominally calcium-free. Under this condition, ATP did not affect the frequency, amplitude and cumulative amplitude of cadmium sIPSCs (Figure 9A–C). Thus, calcium influx from the extracellular space into Purkinje cells is necessary for the suppression of the GABAergic synaptic transmission by ATP.
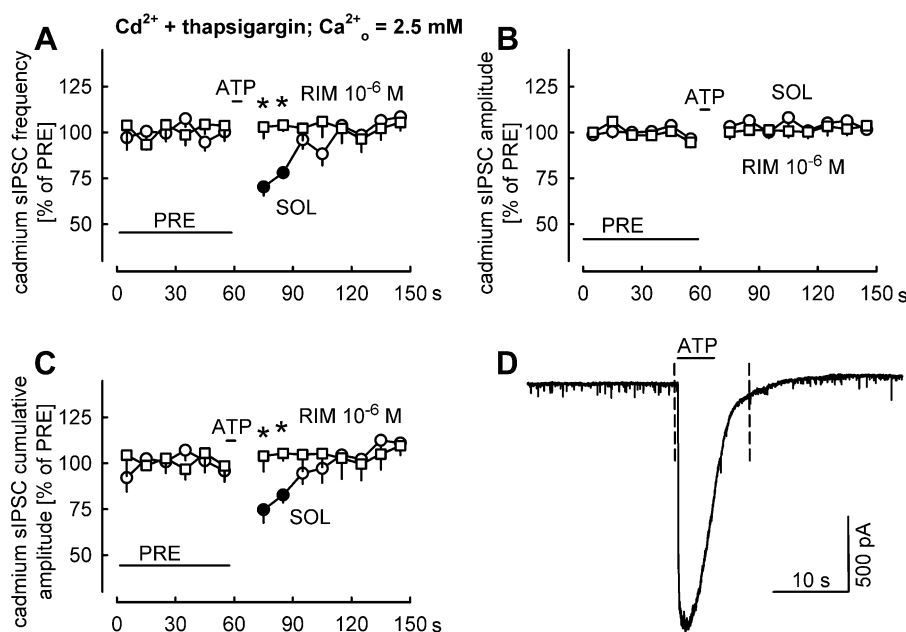
Figure 8

ATP suppresses sIPSCs recorded in the presence of cadmium and thapsigargin. In addition to DNQX and AP5, cadmium (10^{-4} M) and thapsigargin (10^{-5} M) were present in the superfusion ACSF. The experiments in Figures 8 and 9 were performed on the same neurones. Figure 8 shows the first part of the experiment, in which an ACSF with normal calcium concentration was superfused. Figure 9 shows the second part of the experiments, during which calcium-free ACSF was superfused. (A–C) The frequency, amplitude and cumulative amplitude of cadmium sIPSCs were evaluated in 10-s periods and expressed as percentages of values during the initial reference period PRE. Pressure ejection of ATP evoked purinergic currents, but calcium spikes were prevented by cadmium in the ACSF (see D). Means ± standard error of the mean of 12 (SOL) and 10 (RIM) experiments. Filled symbols indicate significant difference versus PRE ($P < 0.05$); * indicates significant difference from SOL ($P < 0.05$). (D) An original tracing recorded in the presence of solvent (the period between the dashed lines was not evaluated in A–C).

The recordings of the present study were performed at room temperature (20–24°C). It is known that the magnitude and duration of endocannabinoid-mediated retrograde signalling changes with temperature (see e.g. Kreitzer and Regehr, 2001). We wanted to verify that ATP is also able to suppress synaptic transmission at more physiological temperatures. The brain slices were superfused at 34°C with ACSF containing cadmium (10^{-4} M) and thapsigargin (10^{-5} M). ATP, pressure ejected as in all previous experiments, lowered the frequency and the cumulative amplitude of cadmium sIPSCs, whereas it did not change their amplitude (supporting Figure S4). The ATP effects appeared to be smaller and delayed compared with the ATP effects at room temperature. Rimonabant prevented the effects of ATP. When the same experiments were carried out in calcium-free ACSF, ATP did not suppress the cadmium sIPSCs (not shown). These results indicate that ATP suppresses GABAergic transmission in a CB$_1$ receptor-dependent manner also at physiological temperatures, albeit with different kinetics than at room temperature.

Discussion

The present study shows for the first time that ATP, very probably by activating P2X purine receptors, elicits endocannabinoid- and CB$_1$ receptor-mediated retrograde sup-

pression of synaptic transmission. Calcium increase in the postsynaptic neurone was necessary for triggering endocannabinoid production and retrograde signalling. ATP induced a calcium increase in the postsynaptic Purkinje cells by two mechanisms. Calcium entered into the Purkinje cells directly via P2X purine receptor ion channels. In addition, depolarization of Purkinje cells after activation of P2X receptors opened voltage-gated calcium channels.

The CB$_1$ receptor antagonist rimonabant (Rinaldi-Carmona *et al.*, 1994; Pertwee, 2005) consistently abolished in several series of experiments the ATP-evoked suppression of the GABAergic synaptic input to the Purkinje cells. This observation points to the involvement of endocannabinoids and CB$_1$ receptors in the suppression.

The analysis of ATP effects on mIPSCs recorded in the presence of tetrodotoxin or on sIPSCs recorded in the presence of cadmium suggests that presynaptic receptors on axon terminals of interneurones were involved in the ATP-evoked suppression of GABAergic synaptic transmission. Thus, ATP did not change the amplitude of mIPSCs or cadmium sIPSCs arguing against a postsynaptic interference with the effect of released GABA. The fact that ATP suppressed the frequency of mIPSCs and of cadmium sIPSCs indicates inhibition of GABA release from the axon terminals. The results of neuroanatomical studies are in agreement with a presynaptic action: axon terminals of GABAergic interneurones in the cerebellar cortex possess CB$_1$ receptors, whereas the postsynaptic Purkinje cells
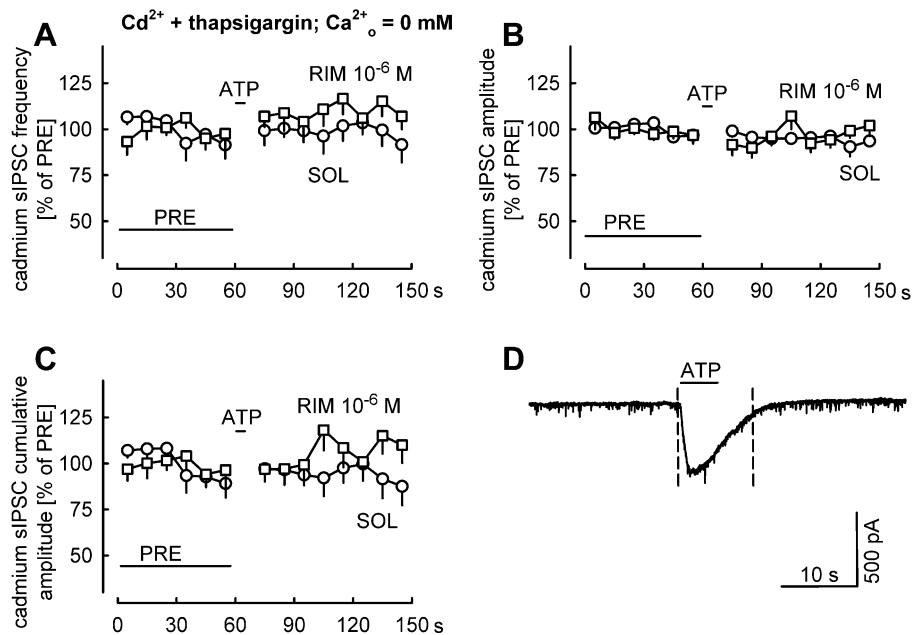
Figure 9

ATP does not suppress sIPSCs recorded in the presence of cadmium and thapsigargin and calcium-free ACSF. In addition to DNQX and AP5, cadmium (10^{-4} M) and thapsigargin (10^{-5} M) were present in the calcium-free superfusion ACSF. Figure 8 shows the first part of the experiment, during which ACSF with normal calcium concentration was superfused. (A–C) The frequency, amplitude and cumulative amplitude of cadmium sIPSCs were evaluated in 10-s periods and expressed as percentages of values during the initial reference period PRE. Means $\pm$ standard error of the mean of 12 (SOL) and 10 (RIM) experiments. (D) An original tracing recorded in the presence of solvent (the period between the dashed lines was not evaluated in A–C).

are largely devoid of CB$_1$ receptors (Tsou *et al.*, 1998; Diana *et al.*, 2002). Exogenous cannabinoids acting on CB$_1$ receptors on axon terminals of interneurones also inhibit synaptic transmission between interneurones and Purkinje cells (e.g. Diana *et al.*, 2002; Szabo *et al.*, 2004).

Several observations indicated that ATP activates P2X purinergic receptors in the Purkinje cells. Thus, the experiments with the ecto-nucleotidase inhibitor ARL67156 indicated that ATP itself elicited the purinergic current, not its degradation products generated by ecto-nucleotidases. The purinergic current was not sensitive to an intracellular activator of G proteins, GTPγS, arguing against the involvement of G protein-coupled receptors in the ATP effect. The involvement of the G protein-coupled A1 receptor in the ATP-evoked current was specifically excluded by using the antagonist DPCPX. Because of a lack of selective antagonists, the P2X receptor subtype was not definitively identified. However, the resistance of the ATP effect to PPADS and the enhancement by ivermectin are compatible with a role for P2X$_4$ receptors. In addition, anatomical receptor localization studies showed the presence of mRNA and protein of several types of P2X receptors in Purkinje cells, including P2X$_4$ receptors (Collo *et al.*, 1996; for review see Nörenberg and Illes, 2000; Rubio and Soto, 2001; Xiang and Burnstock, 2005; Lein *et al.*, 2007).

Several P2X receptors are also permeable to calcium ions in addition to sodium and potassium ions (e.g. Rogers and Dani, 1995; Egan and Khakh, 2004). Hence, it would be expected that the charge carriers of the large inward current evoked by ATP were partly calcium ions. The fluorometrically

measured intracellular calcium concentration increased after ATP application, and a significant portion of this increase persisted when voltage-gated calcium channels were blocked by cadmium, and intracellular calcium stores were depleted by thapsigargin. Importantly, the ATP-evoked purinergic current and the intracellular calcium increase in the dendrites were greatly attenuated in the presence of a calcium-free extracellular buffer. Therefore, it is very likely that ATP activated P2X receptors with a resulting calcium influx through these receptor channels. Very similarly, ATP elicited a P2X receptor-mediated increase in calcium concentration in Purkinje cells in the study of Mateo *et al.* (1998). Undoubtedly, calcium also entered into the postsynaptic neurones via voltage-gated calcium channels, which were activated by ATP-evoked depolarization in distal dendrites escaping voltage-clamp.

As shown by the experiments with the calcium chelator BAPTA, an increased calcium concentration in postsynaptic Purkinje cells was necessary for triggering the ATP-evoked suppression of synaptic transmission. The ATP-evoked suppression of synaptic transmission also operated when calcium influx through voltage-gated calcium channels and calcium release from intracellular stores were inactivated, supporting the hypothesis that calcium influx via P2X receptors is sufficient for triggering endocannabinoid production. In strong support for the role of calcium influx via P2X receptors in the suppression of the GABAergic synaptic transmission is the observation that ATP did not evoke suppression when the extracellular calcium concentration was nominally zero.

Abolishment of the ATP-evoked suppression of GABAergic synaptic transmission by BAPTA rules out the possibility that ATP (or its degradation products) lowered GABA release by a direct action on GABAergic axon terminals. It was reported that ATP elicits 2-arachidonoylglycerol release from microglial cells (Witting *et al.*, 2004). Prevention of ATP-evoked suppression of GABAergic transmission by BAPTA in the Purkinje cells makes it also unlikely that ATP primarily acted on glial cells and 2-arachidonoylglycerol released by glial cells inhibited the GABA release from the axon terminals.

It is theoretically possible that ATP (or a degradation product of ATP) activated $G\alpha_{q/11}$ protein-coupled P2Y receptors on Purkinje cells, thus triggering endocannabinoid production and endocannabinoid-mediated retrograde suppression of GABA release from interneurone axon terminals, similar to the manner in which activated mGluR1 receptors lead to retrograde signalling (e.g. Galante and Diana, 2004). One argument against the involvement of $G\alpha_{q/11}$ protein-coupled P2Y receptors is that the ATP-evoked current was insensitive to GTPγS. A further argument against the involvement of $G\alpha_{q/11}$ protein-coupled P2Y receptors is that the ATP-evoked retrograde signalling was prevented by BAPTA in the postsynaptic Purkinje cells. $G\alpha_{q/11}$ protein-mediated retrograde signalling between Purkinje cells and their afferent axons continues to operate when calcium in Purkinje cells is kept low by BAPTA (Maejima *et al.*, 2001; Galante and Diana, 2004). Notably, at synapses in other brain areas, $G\alpha_{q/11}$ protein-mediated endocannabinoid production and retrograde signalling can be blocked by buffering calcium in the postsynaptic neurones (Kushmerick *et al.*, 2004; Kola *et al.*, 2008).

Altogether, the participation of CB_1 receptors, the involvement of presynaptic inhibition and the results of the BAPTA-, cadmium- and calcium-free ACSF experiments support the following mode of retrograde signalling: ATP acts on P2X purine receptors on postsynaptic Purkinje cells, calcium concentration increases due to calcium influx via P2X receptors and via voltage-gated calcium channels, endocannabinoids are released, and retrogradely diffusing endocannabinoids inhibit GABA release from presynaptic axon terminals. Retrograde signalling between Purkinje cells and interneurone axon terminals has been repeatedly shown in the past: calcium influx through voltage-gated calcium channels and activity of $G\alpha_{q/11}$ protein-coupled receptors were the triggers of endocannabinoid production (Diana *et al.*, 2002; Brenowitz and Regehr, 2003; Diana and Marty, 2003; Szabo *et al.*, 2004, 2006).

Interneurones of the cerebellar cortex possess somatodendritic P2X- and P2Y-receptors. Acting on these receptors, ATP and its degradation products enhance the firing of the interneurones and – consequently – the frequency and amplitude of GABAergic sIPSCs recorded in Purkinje cells (Brockhaus *et al.*, 2004; Saitow *et al.*, 2005; Deitmer *et al.*, 2006). We studied the effect of ATP on mIPSCs isolated by tetrodotoxin and on sIPSCs isolated by cadmium. Tetrodotoxin and cadmium strongly impede the coupling between the soma and the axon terminals of interneurones (but a weak electrotonic coupling may persist in the presence of these agents; Glitsch and Marty, 1999). Thus, it is unlikely that the somatodendritic stimulant ATP effects confounded the inhibitory ATP effects on the axon terminals of interneurones.

Donato *et al.* (2008) observed a presynaptic inhibition of interneurone – Purkinje cell transmission by the antagonist PPADS and after desensitization of P2X receptors. It was assumed that endogenous ATP tonically activates P2X receptors on axon terminals of GABAergic interneurones. In our experiments, ATP did not increase the frequency of mIPSCs or cadmium sIPSCs even in the presence of the CB_1 antagonist rimonabant. The reason for this discrepancy between our results and the results of Donato *et al.* (2008) is not known. It is notable, however, that we directly studied the effect of ATP, whereas Donato *et al.* (2008) studied the effects of ATP antagonists. Compatible with our observations, Brockhaus *et al.* (2004) also did not see an ATP-evoked enhancement of mIPSC frequency in Purkinje cells.

We have shown that activation of P2X transmitter-gated ion channels leads to calcium-dependent and CB_1 receptor-dependent retrograde signalling. Although endocannabinoids were not chemically detected in the present study, it is very likely that the retrograde signalling was mediated by endocannabinoids produced by postsynaptic Purkinje cells. It has been shown previously by biochemical measurements that activation of P2X receptors leads to endocannabinoid production; ATP elicited the release of 2-arachidonoylglycerol in cultivated microglial cells (Witting *et al.*, 2004). Our electrophysiological experiments showed that activation of neuronal P2X purine receptors can also lead to endocannabinoid production. The number of publications on the involvement of transmitter-gated ion channels in endocannabinoid production is limited. Thus, Ohno-Shosaku *et al.* (2007) showed that activation of NMDA-type ionotropic glutamate receptors leads to calcium-dependent 2-arachidonoylglycerol production and retrograde suppression of GABAergic synaptic transmission between cultivated hyppocampal neurones. Until recently, calcium influx through voltage-gated calcium channels and activity of $G\alpha_{q/11}$ protein-coupled receptors were regarded as triggers of endocannabinoid production in postsynaptic neurones. The study of Ohno-Shosaku *et al.*, (2007) and our study show that calcium influx via transmitter-gated ion channels is a third possibility for triggering endocannabinoid production and endocannabinoid-mediated retrograde synaptic signalling. It is noteworthy that at the resting membrane potential, P2X receptors may serve – in contrast to NMDA receptors – as major calcium entry pathways, because they are not blocked by magnesium under this condition.

Do our observations possess a (patho)physiological relevance? ATP is released in the central nervous system by both exocytotic and non-exocytotic mechanisms, and especially neuronal injury or neurodegenerative processes lead to a massive outflow of ATP (Burnstock, 2006). It is conceivable that under these conditions, ATP elicits endocannabinoid release and suppresses the release of inhibitory, but also excitatory, transmitters.

Acknowledgements

Conflicts of interest

The authors state no conflict of interest.

References

Abbracchio MP, Burnstock G (1994). Purinoceptors: are there families of P2X and P2Y purinoceptors? Pharmacol Ther 64: 445–475.

Abbracchio MP, Burnstock G, Boeynaems J-M, Barnard EA, Boyer JL, Kennedy C et al. (2006). International union of pharmacology LVIII: update on the P2Y G protein-coupled nucleotide receptors: from molecular mechanism and pathophysiology to therapy. Pharmacol Rev 58: 281–341.

Alexander SPH, Mathie A, Peters JA (2009). Guide to receptors and channels (GRAC), 4th edn. Br J Pharmacol 158 (Suppl. 1): S1–S254.

Alger BE (2002). Retrograde signaling in the regulation of synaptic transmission: focus on endocannabinoids. Prog Neurobiol 68: 247–286.

Brenowitz SD, Regehr WG (2003). Calcium dependence of retrograde inhibition by endocannabinoids at synapses onto Purkinje cells. J Neurosci 23: 6373–6384.

Brenowitz SD, Best AR, Regehr WG (2006). Sustained elevation of dendritic calcium evokes widespread endocannabinoid release and suppression of synapses onto cerebellar Purkinje cells. J Neurosci 26: 6841–6850.

Brockhaus J, Dressel D, Herold S, Deitmer JW (2004). Purinergic modulation of synaptic input to Purkinje neurons in rat cerebellar brain slices. Eur J Neurosci 19: 2221–2230.

Brown SP, Brenowitz SD, Regehr WG (2003). Brief presynaptic bursts evoke synapse-specific retrograde inhibition mediated by endogenous cannabinoids. Nat Neurosci 6: 1048–1057.

Buell G, Lewis C, Collo G, North RA, Surprenant A (1996). An antagonist-insensitive P_{2X} receptor experessed in epithelia and brain. EMBO J 15: 55–62.

Burnstock G (2006). Pathophysiology and therapeutic potential of purinergic signaling. Pharmacol Rev 58: 58–86.

Burnstock G (2007). Purine and pyrimidine receptors. Cell Mol Life Sci 64: 1471–1483.

Chevaleyre V, Takahashi KA, Castillo PE (2006). Endocannabinoid-mediated synaptic plasticity in the CNS. Annu Rev Neurosci 29: 37–75.

Collo G, North RA, Kawashima E, Merlo-Pitch E, Niedhart S, Surprenant A et al. (1996). Cloning of $P2X_5$ and $P2X_6$ receptors and the distribution and properties of an extended family of ATP-gated ion channels. J Neurosci 16: 2495–2507.

Deitmer JW, Brockhaus J, Casel D (2006). Modulation of synaptic activity in Purkinje neurons by ATP. Cerebellum 5: 49–54.

Di Angelantonio S, Nistri A (2001). Calibration of agonist concentrations applied by pressure pulses or via rapid solution exchanger. J Neurosci Methods 110: 155–161.

Diana MA, Marty A (2003). Characterization of depolarization-induced suppression of inhibition using paired interneuron-Purkinje cell recordings. J Neurosci 23: 5906–5918.

Diana MA, Levenes C, Mackie K, Marty A (2002). Short-term retrograde inhibition of GABAergic synaptic currents in rat Purkinje cells is mediated by endogenous cannabinoids. J Neurosci 22: 200–208.

Donato R, Rodrigues RJ, Takahashi M, Chi M, Soto D, Miyagi K et al. (2008). GABA release by basket cells onto Purkinje cells, in rat cerebellar slices, is directly controlled by presynaptic receptors, modulating Ca^{2+} influx. Cell Calcium 44: 521–532.

Egan TM, Khakh BS (2004). Contribution of calcium ions to P2X channel responses. J Neurosci 24: 3413–3420.

Fortin DA, Trettel J, Levine ES (2004). Brief trains of action potentials enhance pyramidal neuron excitability via endocannabinoid-mediated suppression of inhibition. J Neurophysiol 92: 2105–2112.

Fredholm BB, Abbracchio MP, Burnstock G, Dubyak GR, Harden KT, Jacobson KA et al. (1997). Towards a revised nomenclature for P1 and P2 receptors. Trends Pharmacol Sci 18: 79–82.

Freiman I, Anton A, Monyer H, Urbanski MJ, Szabo B (2006). Analysis of the effects of cannabinoids on identified synaptic connections in the caudate-putamen by paired recordings in transgenic mice. J Physiol 575: 789–806.

Freund TF, Katona I, Piomelli D (2003). Role of endogenous cannabinoids in synaptic signaling. Physiol Rev 83: 1017–1066.

Galante M, Diana MA (2004). Group I metabotropic glutamate receptors inhibit GABA release at interneuron - Purkinje cell synapses through endocannabinoid production. J Neurosci 24: 4865–4874.

Gever JR, Cockayne DA, Dillon MP, Burnstock G, Ford APDW (2006). Pharmacology of P2X channels. Pflugers Arch 452: 513–537.

Glitsch M, Marty A (1999). Presynaptic effects of NMDA in cerebellar Purkinje cells and interneurons. J Neurosci 19: 511–519.

Howlett AC, Barth F, Bonner TI, Cabral G, Casellas P, Devane WA et al. (2002). International union of pharmacology. XXVII. Classification of cannabinoid receptors. Pharmacol Rev 54: 161–202.

Illes P, Nieber K, Nörenberg W (1996). Electrophysiological effects of ATP on brain neurons. Auton Pharmacol 16: 407–411.

Jarvis MF, Khakh BF (2009). ATP-gated P2X cation channels. Neuropharmacol 56: 208–215.

Jeong H-J, Han S-H, Min B-I, Cho Y-W (2001). 5-HT$_{1A}$ receptor-mediated activation of G-protein-gated inwardly rectifying K^+ current in rat periaqueductal gray neurons. Neuropharmacol 41: 175–185.

Jones CA, Chessell IP, Simon J, Barnard EA, Miller KJ, Michel AD et al. (2000). Functional characterization of the $P2X_4$ receptor orthologues. Br J Pharmacol 129: 388–394.

Kano M, Ohno-Shosaku T, Hashimotodani Y, Uchigashima M, Watanabe M (2009). Endocannabinoid-mediated control of synaptic transmission. Physiol Rev 89: 309–380.

Kim J, Alger BE (2004). Inhibition of cyclooxygenase-2 potentiates retrograde endocannabinoid effects in hippocampus. Nat Neurosci 7: 697–698.

Kim SJ, Kim YS, Yuan JP, Petralia RS, Worley PF, Linden DJ (2003). Activation of the TRPC1 cation channel by metabotropic glutamate receptor mGluR1. Nature 426: 285–291.

Klotz KN (2000). Adenosine receptors and their ligands. Naunyn Schmiedebergs Arch Pharmacol 362: 382–391.

Kola B, Farkas I, Christ-Crain M, Wittmann G, Lolli F, Amin F *et al.* (2008). The orexigenic effect of ghrelin is mediated through central activation of the endogenous cannabinoid system. PLoS ONE 3: e1797.

Kreitzer AC, Regehr WG (2001). Retrograde inhibition of presynaptic calcium influx by endogenous cannabinoids at excitatory synapses onto Purkinje cells. Neuron 29: 717–727.

Kushmerick C, Price GD, Taschenberger H, Puente N, Renden R, Wadiche JI *et al.* (2004). Retroinhibition of presynaptic Ca²⁺ currents by endocannabinoids released via postsynaptic mGluR activation at a calyx synapse. J Neurosci 24: 2955–2965.

Lambrecht G (2000). Agonists and antagonists acting at P2X receptors: selectivity profiles and functional implications. Naunyn Schmiedebergs Arch Pharmacol 362: 340–350.

Lasser-Ross N, Ross WN (1992). Imaging voltage and synaptically activated sodium transients in cerebellar Purkinje cells. Proc R Soc Lond 247: 35–39.

Lein ES, Hawrylycz MJ, Ao N, Ayres M, Bensinger A, Bernard A *et al.* (2007). Genome-wide atlas of gene expression in the adult mouse brain. Nature 445: 168–176.

Lovinger DM (2008). Presynaptic modulation by endocannabinoids. In: Südhof TC, Starke K (eds). Pharmacology of Neurotransmitter Release. Handbook of Experimental Pharmacology, Vol. 184. Springer Press: Berlin, Heidelberg, pp. 435–477.

Maejima T, Hashimoto K, Yoshida T, Aiba A, Kano M (2001). Presynaptic inhibition caused by retrograde signal from metabotropic glutamate to cannabinoid receptors. Neuron 31: 463–475.

Maejima T, Oka S, Hashimotodani Y, Ohno-Shosaku T, Aiba A, Wu D *et al.* (2005). Synaptically driven endocannabinoid release requires Ca²⁺-assisted metabotropic glutamate receptor subtype 1 to phospholipase C β4 signaling cascade in the cerebellum. J Neurosci 25: 6826–6835.

Marcaggi P, Attwell D (2005). Endocannabinoid signaling depends on the spatial pattern of synapse activation. Nat Neurosci 8: 776–781.

Mateo J, Garcia-Lecea M, Miras-Portugal MT, Castro E (1998). Ca²⁺ signals mediated by P2X-type purinoceptors in cultured cerebellar Purkinje cells. J Neurosci 18: 1704–1712.

Nörenberg W, Illes P (2000). Neuronal P2X receptors: localisation and functional properties. Naunyn Schmiedebergs Arch Pharmacol 362: 324–339.

North RA (2002). Molecular physiology of P2X receptors. Physiol Rev 82: 1013–1067.

Ohno-Shosaku T, Hashimotodani Y, Ano M, Takeda S, Tsubokawa H, Kano M (2007). Endocannabinoid signalling triggered by NMDA receptor-mediated calcium entry into rat hippocampal neurons. J Physiol 584: 407–418.

Pertwee RG (2005). Pharmacological actions of cannabinoids. In: Pertwee R (ed.). Cannabinoids. Handbook of Experimental Pharmacology, Vol. 168. Springer Press: Berlin, Heidelberg, New York, pp. 1–51.

Ralevic V, Burnstock G (1998). Receptors for purines and pyrimidines. Pharmacol Rev 50: 413–492.

Rancz EA, Häusser M (2006). Dendritic calcium spikes are tunable triggers of cannabinoid release and short-term synaptic plasticity in cerebellar Purkinje neurons. J Neurosci 26: 5428–5437.

Rinaldi-Carmona M, Barth F, Heaulme M, Shire D, Calandra B, Congy C *et al.* (1994). SR141716A, a potent and selective antagonist of the brain cannabinoid receptor. FEBS Lett 350: 240–244.

Rogers M, Dani JA (1995). Comparison of quantitative calcium flux through NMDA, ATP, and Ach receptor channels. Biophys J 68: 501–506.

Rubio ME, Soto F (2001). Distinct localization of P2X receptors at excitatory postsynaptic specializations. J Neurosci 21: 641–653.

Saitow F, Murakoshi T, Suzuki H, Konishu S (2005). Metabotropic P2Y purinoceptor-mediated presynaptic and postsynaptic enhancement of cerebellar GABAergic transmission. J Neurosci 23: 2108–2116.

Stephens GJ (2009). G-protein-coupled-receptor-mediated presynaptic inhibition in the cerebellum. Trends Pharmacol Sci 630: 421–430.

Straiker A, Mackie K (2007). Metabotropic suppression of excitation in murine autaptic hippocampal neurons. J Physiol 578: 773–785.

Stuart G, Häusser M (1994). Initiation and spread of sodium action potentials in cerebellar Purkinje cells. Neuron 13: 703–712.

Szabo B, Schlicker E (2005). Effects of cannabinoids on neurotransmission. In: Pertwee R (ed.). Cannabinoids. Handbook of Experimental Pharmacology, Vol. 168. Springer Press: Berlin, Heidelberg, New York, pp. 327–365.

Szabo B, Than M, Thorn D, Wallmichrath I (2004). Analysis of the effects of cannabinoids on synaptic transmission between basket and Purkinje cells in the cerebellar cortex of the rat. J Pharmacol Exp Ther 310: 915–925.

Szabo B, Urbanski MJ, Bisogno T, Di Marzo V, Mendiguren A, Bär W *et al.* (2006). Depolarization-induced retrograde synaptic inhibition in the cerebellar cortex is mediated by 2-arachidonoylglycerol. J Physiol (Lond) 577: 263–280.

Than M, Szabo B (2002). Analysis of the function of $GABA_B$ receptors on inhibitory afferent neurons of Purkinje cells in the cerebellar cortex of the rat. Eur J Neurosci 15: 1575–1584.

Townsend-Nicholson A, King BF, Wildman SS, Burnstock G (1999). Molecular cloning, functional characterization and possible cooperativity between the murine $P2X_4$ and $P2X_{4a}$ receptors. Mol Brain Res 64: 246–254.

Tsou K, Brown S, Sanudo-Pena MC, Mackie K, Walker JM (1998). Immunohistochemical distribution of cannabinoid CB1 receptors in the rat central nervous system. Neuroscience 83: 393–411.

Varma N, Carlson GC, Ledent C, Alger BE (2001). Metabotropic glutamate receptors drive the endocannabinoid system in hippocampus. J Neurosci 21: RC188.

Von Kügelgen I (2006). Pharmacological profiles of cloned mammalian P2Y-receptor subtypes. Pharmacol Ther 110: 415–432.

Wallmichrath I, Szabo B (2002). Cannabinoid inhibit striatonigral GABAergic neurotransmission in the mouse. Neuroscience 113: 671–682.

Wilson RI, Nicoll RA (2001). Endogenous cannabinoids mediate retrograde signalling at hippocampal synapses. Nature 410: 588–592.

Witting A, Walter L, Wacker J, Möller T, Stella N (2004). P2X7 receptors control 2-arachidonoylglycerol production by microglial cells. Proc Natl Acad Sci USA 101: 3214–3219.

Xiang Z, Burnstock G (2005). Changes in expression of P2X purinoceptors in rat cerebellum during postnatal development. Brain Res Dev Brain Res 156: 147–157.

Zimmermann H (1996). Biochemistry, localisation and functional roles of ecto-nucleotidase in the nervous system. Prog Neurobiol 49: 589–618.

Supporting information

Additional Supporting Information may be found in the online version of this article:

Figure S1 PPADS does not affect the ATP-evoked currents. In addition to DNQX, AP5 and bicuculline, cadmium was added to the superfusion ACSF to block voltage-gated calcium channels. ATP was pressure ejected from a pipette. For obtaining concentration-response relationships, the duration of the pressure pulse was varied (0.1–5 s). In each experiment, two concentration-response curves were obtained. Current amplitudes were expressed as percentages of the current obtained at the 5 s pressure pulse within the first concentration-response curve (this first curve is called PRE). (A) After the first concentration-response curve (PRE) the second curve was obtained in the presence of solvent (SOL). Means ± SEM of 3 experiments are shown. (B) After the first concentration-response curve (PRE) the second curve was obtained in the presence of the mixed P2X/P2Y antagonist PPADS (10^{-4} M). Means ± SEM of 7 experiments are shown. (B2-B3) Original tracings of ATP-evoked currents during PRE and during PPADS superfusion.

Figure S2 Effects of ATP on cumulative probability distribution plots of mIPSC amplitudes and inter-event intervals. In addition to DNQX and AP5, tetrodotoxin (3×10^{-7} M) was present in the superfusion ACSF to block voltage-gated sodium channels. ATP evoked purinergic currents which were accompanied by calcium spikes. The plots were constructed using 20-s periods preceding (PRE) and following ATP application (after ATP) in one of the experiments shown in Figure 6. Bins for amplitudes and inter-event intervals were

multiples of 10 pA and 50 ms respectively. *Indicates significant difference ($P < 0.05$) between the distribution plots identified by the Kolmogorov-Smirnov test.

Figure S3 BAPTA prevents the suppression of mIPSCs by ATP. In addition to DNQX and AP5, tetrodotoxin (3×10^{-7} M) was present in the superfusion ACSF to block voltage-gated sodium channels. The patch-clamp pipette contained the calcium chelator BAPTA (4×10^{-2} M). (A–C) The frequency, amplitude and cumulative amplitude of mIPSCs were evaluated in 10-s periods and expressed as percentages of values during the initial reference period PRE. Pressure ejection of ATP evoked purinergic currents which were accompanied by calcium spikes (see D). Means ± standard error of the mean of 17 (SOL) and 17 (RIM) experiments are shown. (D) An original tracing recorded in the presence of solvent (the period between the dashed lines was not evaluated in A–C).

Figure S4 ATP suppresses sIPSCs recorded in the presence of cadmium and thapsigargin also at 34°C. In addition to DNQX and AP5, cadmium (10^{-4} M) and thapsigargin (10^{-5} M) were present in the superfusion ACSF. (A–C) The frequency, amplitude and cumulative amplitude of cadmium sIPSCs were evaluated in 10-s periods and expressed as percentages of values during the initial reference period PRE. Pressure ejection of ATP evoked purinergic currents, but calcium spikes were prevented by cadmium in the ACSF (see D). Means ± standard error of the mean of 15 (SOL) and 15 (RIM) experiments are shown. Filled symbols indicate significant difference versus PRE ($P < 0.05$); * indicates significant difference from SOL ($P < 0.05$). (D) An original tracing recorded in the presence of solvent (the period between the dashed lines was not evaluated in A–C).

Please note: Wiley-Blackwell are not responsible for the content or functionality of any supporting materials supplied by the authors. Any queries (other than missing material) should be directed to the corresponding author for the article.